ACS APPLIED MATERIALS & INTERFACES

Research Article

www.acsami.org

Spin-Assisted Multilayers of Poly(methyl methacrylate) and Zinc Oxide Quantum Dots for Ultraviolet-Blocking Applications

Mohamed Eita,*[,†] Lars Wågberg,[‡,§] and Mamoun Muhammed[†]

[†]Division of Functional Materials (FNM), Royal Institute of Technology (KTH), SE-16440 Kista-Stockholm, Sweden

[‡]Department of Polymer and Fibre Technology, Royal Institute of Technology (KTH), Teknikringen 56, SE-10044 Stockholm, Sweden

[§]Wallenberg Wood Science Centre, Teknikringen 56, SE-10044 Stockholm, Sweden

Supporting Information

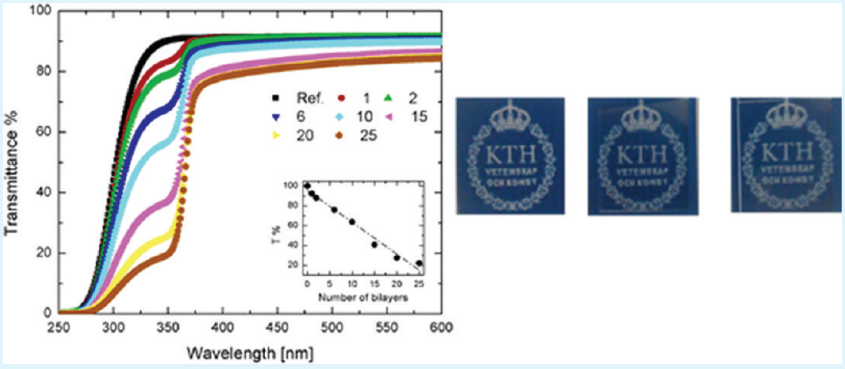

ABSTRACT: Thin UV-blocking films of poly(methyl methacrylate) (PMMA) and ZnO quantum dots (QDs) were built-up by spin-coating. Ellipsometry reveals average thicknesses of 9.5 and 8.6 nm per bilayer before and after heating at 100 °C for one hour, respectively. The surface roughness measured by Atomic force microscopy (AFM) was 3.6 and 8.4 nm for the one and ten bilayer films, respectively. The linear increase in thickness as well as the low surface roughness increment per bilayer indicates a stratified multilayer structure and a smooth interface without aggregation. The absorption of UV radiation increased with increasing number of bilayers. At the same time, transmission was damped at wavelengths shorter than 375 nm. The thin films had a high and constant transparency in the visible region. Green-light emitting QDs could be detected by confocal microscopy at a concentration of 20% in a single layer of PMMA/ZnO. PMMA/ZnO QDs thin films are hydrophobic, as indicated by contact angle measurements.

KEYWORDS: *transmission, absorption, radiation, transparency, emission, layer*

INTRODUCTION

UV radiation is found in sunlight at wavelengths of 100−400 nm and is divided into three major regions; UVA (400−315 nm), UVB (315−280 nm) and UVC (280−100 nm).[1] Recent studies have demonstrated that large amounts of UVB radiation can cause damage and rearrangement in the DNA of plants.[2] Therefore, the scientific community has paid considerable attention to developing materials that are able to block or reduce UV transmission in these regions of radiation. Materials containing UV-absorbing materials and polymers of high transparency are promising for UV-blocking applications.[3] Combining nanoparticles and polymers into nanocomposites opens the way for a broad range of interesting properties and applications.[4] ZnO is a direct band gap semiconductor (3.3 eV) and absorbs radiation in the UV region, and it is therefore of interest as a UV-absorbing material in such nanocomposites.[5−8] Poly(methyl methacrylate) PMMA is suitable for UV-blocking applications since it has a high transparency throughout the visible range in addition to high mechanical stability which promotes the use of these nanocomposites in the relevant applications.[9,10] UV-blocking nanocomposites have been manufactured by different routes.[11−18] A combination of ZnO and PMMA led to a full blocking of the UV radiation in the 290−340 nm range, and the PMMA blocked the radiation in the 200−280 nm range, but the whole composite showed a reasonable transparency in the visible region.[19] Thin ZnO/PMMA films fabricated by either dip- or spin-coating from a ZnO/PMMA mixture prepared by the sol−gel process possess a high degree of orientation of the ZnO nanoparticles and exhibit an increasing UV absorption with increasing number of layers.[20] Mechanical blending has also been used to prepare ZnO/PMMA nanocomposites which show a crystalline hexagonal structure and an increasing UV absorption with increasing ZnO content.[21] Furthermore, solution casting was

Received: February 11, 2012
Accepted: May 29, 2012
Published: May 29, 2012

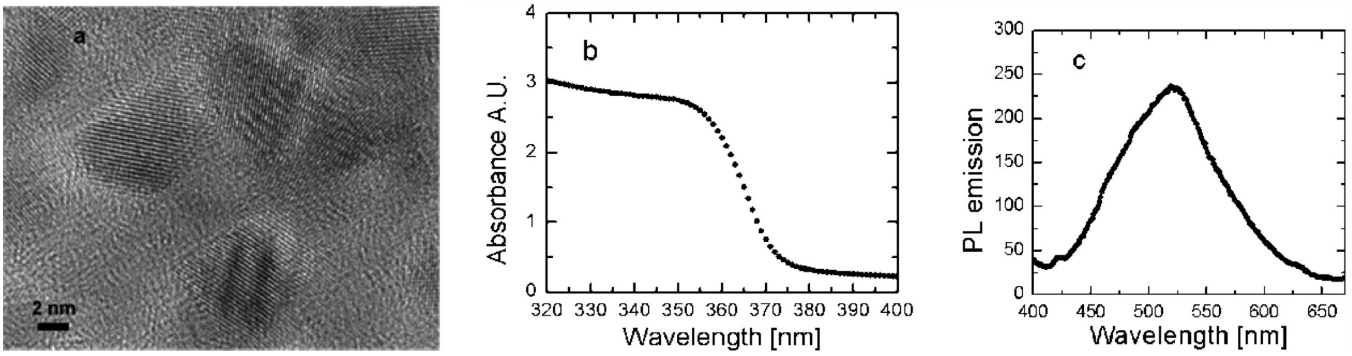

Figure 1. (a) HRTEM image indicating a size ≤5 nm, (b) UV absorption spectrum showing an absorption shoulder at about 351 nm, and (c) photoluminescence emission spectrum showing emission peak at 522 nm of the ZnO QDs dispersed in toluene.

used to prepare a nanocomposite containing polystyrene (PS) which as a matrix polymer resulted in an ordered structure that blocked the UV radiation and afforded a high degree of transparency which decreased with increasing ZnO content.[22] Both PSS and PMMA were used as a flowing liquid in front of a ZnO oxide target to be sputtered by focused pulsed laser ablation to form a nanocomposite after drying of the solvent.[23] In a previous study, we have demonstrated that thin films of ZnO nanoparticles and poly(acrylic acid) (PAA) prepared by dip-coating show a UV-blocking feature in addition to broad-band antireflective properties in the visible region and extending into the near-infrared region.[24] The high transparency shown by these thin films was considered to be related to the high porosity of the film which at the same time resulted in another interesting feature of superhydrophilicity.[24]

Due to the quantum confinement, ZnO Quantum dots (QDs) show interesting features of photoluminescence emission and high quantum yield in addition to photostability in dispersions.[25] QDs are also characterized by a size-dependent photoluminescent emission, which results in different emission colors for different dot sizes when they are excited at a given wavelength.[26] To utilize the excellent optical properties of QDs, they have to be evenly distributed on the surface or inside the polymer matrix. In this respect, spin coating is a rather facile method to coat a monolayer of either polymers or nanoparticles. It can be used to build up multilayers of noncharged molecules dissolved in organic solvents as an alternative to the layer-by-layer technique. Recently, it was shown that multilayers of polyelectrolytes and gold nanoparticles could be built up by spin-coating, resulting in a stratified layer structure with low internal roughness in addition to a constant rate of thickness growth with increasing number of bilayers.[27]

It has been a challenge to produce a broad-band highly transparent UV-blocking material with a controllable UV-blocking efficiency and thickness. The problem in UV-blocking systems prepared so far is that increasing the ZnO content resulted in increasing the opacity of the composite although a high degree of transparency is required. Moreover, most of the reported UV-blocking materials are in the form bulk composites whereas thin films maybe advantageous due to the facile applicability in different systems. In the present work, we have used the spin-coating technique to build up multilayers of ZnO QDs and PMMA in order to fabricate transparent UV-blocking films with controllable UV-blocking efficiency and thickness. Such a method is an alternative to the previously reported methods for manufacturing nanocomopsites of PMMA/ZnO by chemical synthesis. The resulting thin films can be applied directly to a variety of surfaces without the constrains of the nanocomposites or the chemical synthesis. The focus has been on the physical properties and the structural characteristics of the prepared thin films, including the optical and the morphological characterization of the QDS, in order to develop a physical insight into the nature and properties of the resulting material.

EXPERIMENTAL SECTION

Materials. Zinc acetate (reagent grade, Sigma), tetramethylammonium hydroxide (TMAOH, Sigma), oleic acid (Fluka) and PMMA with an average M_w of 350 000 (Alfa Aeser) were used, together with microscope glass slides (Mänzel glässer), and polished silica wafers (p-doped with Boron) from MEMC electronic material.

Preparation of Thin Films. ZnO quantum dots were prepared according to a previously reported scheme[28] by dissolving 660 mg zinc acetate in 60 mL hot ethanol under vigorous stirring. Two-hundred ten microliters of oleic acid was added and the mixture was heated under reflux. Separately, 1.08 g of TMAOH was dissolved in 15 mL of ethanol and injected into the zinc acetate/oleic acid mixture; all the reactants were refluxed for 2 min and then diluted with 150 mL ethanol and cooled, using ice, to 0 °C. ZnO was formed as a white precipitate and collected by ultracentrifugation for 15 min at 4000 rpm; the precipitate was washed several times with ethanol and finally suspended in 30 mL of toluene. PMMA was dissolved in toluene at a concentration of 0.5 wt %. Glass substrates were cleaned by immersion in 0.1 M NaOH for 10 min and then rinsed extensively with ultrapure water and dried with nitrogen. Silica substrates were cleaned by immersion in Piranha solution (3:1 H_2SO_4: H_2O_2) for 20 min followed by extensive rinsing with ultrapure water and were finally dried with nitrogen. Thin films were prepared by spin-coating of PMMA and ZnO QDs in successive steps using a spin-coater from LAURELL Technologies Corporation for 30 s at 3000 rpm. A constant volume of 200 μL of liquid was used; the spinning speed and the spinning time were also kept constant for all the layers. First, a layer of PMMA was coated followed by a layer of ZnO QDs and so in subsequent steps.

Characterization. UV−visible absorbance and transmission spectra were obtained using a Perkin-Elmer Lambda 750 spectrometer. Atomic force microscopy (AFM) images were obtained using a Nanoscope Multimode IIIa microscope, Veeco. Images were taken in the tapping mode at 23 °C and 50% relative humidity. N-doped silica cantilevers with a spring constant of 20−80 N/m were used. High resolution transmission electron microscopy (HRTEM) images were taken by JEOL JEM-2100F at an acceleration voltage of 200 kV. The thicknesses of the multilayers on silica substrates were determined by ellipsometry using a manual nulling photoelectric ellipsometer (Type 43702−200E Rudolph Research) with a mercury lamp at a wavelength of 546.1 nm. Confocal microscope imaging was performed using a Nikon ECLIPSE TE300. Contact angle measurements were made using a CAM 200, KSV instruments Ltd., contact angle goniometer at

room temperature, using Milli-Q water as the liquid in contact with the surface.

RESULTS AND DISCUSSION

Prior to preparing the PMMA/ZnO QDs thin films, the ZnO QDs dispersions were characterized by HRTEM (Figure 1a), UV−vis spectroscopy (Figure 1b), and photoluminescence spectroscopy (Figure 1c). ZnO QDs have a size ≤5 nm as indicated by the HRTEM; they are highly crystalline as indicated by the well-ordered lattice planes at a constant separation of about 0.2 nm. The UV−vis spectrum shows an absorption shoulder at about 351 nm, while the photoluminescence spectrum shows an emission peak at about 522 nm which can be seen as a yellowish green color under a UV lamp. It has been reported elsewhere that the green emission of ZnO QDs is due to recombination of donor−acceptor, where the donors are assumed to be oxygen defects and the acceptors Zn holes.[29−31]The prepared ZnO QDs are confined in size and well dispersed in toluene as a result of the hydrophobicity of the capping oleic acid; they absorb radiation in the UV region and emit their fluorescence in the visible region.

Thin films of PMMA and ZnO QDs were built up by spin coating on silica substrates. The films were heated at 100 °C for one hour to ensure evaporation of the solvent and to homogenize the multilayers. The thickness of these films was measured by ellipsometry. Figure 2 shows the development of

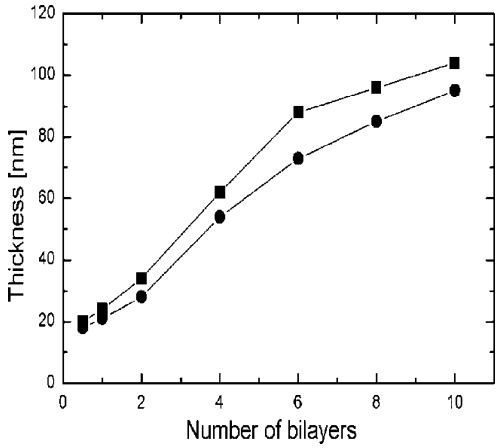

Figure 2. Thickness of PMMA/ZnO QDs thin films prepared by spin-coating on silica substrates before (squares) and after (circles) heating at 100 °C for 1 h.

thickness with increasing number of bilayers before and after heat treatment. The first PMMA layer is presented in the figure as a 0.5 bilayer and shows a thickness of 20 nm, which shrinks to 18 nm after heat treatment. The first bilayer had an initial thickness of 24 nm, which decreased to 21 nm upon heat treatment. This implies that a single layer of ZnO was 4 nm thick before heating and 3 nm thick after heating. A thickness of 4 nm means that the ZnO QDs layer is a uniform monolayer of closely packed QDs without agglomerates. A linear fit of the thickness data results in an average thickness of 9.5 and 8.6 nm per bilayer before and after heat treatment, respectively. Thus the heat treatment has not only helped to remove the solvent but has also caused the film to shrink in a direction normal to the substrate. The results show the efficiency of the spin-coating technique for coating such thin films. The spinning speed plays a crucial role. The speed used to prepare the PMMA/ZnO QDs thin films was 3000 rpm. A lower speed may result in a thicker film and vice versa.

The average thickness per bilayer was evidently less than the first bilayer thickness; which may be attributed to the hydrophobicity of both PMMA and ZnO QDs, because they are coated with oleic acid. The hydrophobicity increases with increasing number of bilayers and affects the monolayer thickness by hindering the spreading of the molecules on the surface. Thus the monolayer thickness may decrease with increasing bilayer number. The morphology of the thin films was investigated by AFM, figure 3, which shows that ZnO QDs are closely packed on the surface of the PMMA layer. However, the size of each particle was apparently greater than that measured by HRTEM, which may indicate an in-plane association of QDs resulting in a size in the AFM image larger than their actual size. Association of QDs during spinning may occur due to the hydrophobicity of PMMA which prevents the fast positioning of particles of the upcoming ZnO layer on the PMMA surface. It can also be seen that each particle is structured, indicating that each associated particle consists of several QDs close to each other. The rms surface roughness of the one bilayer film was 3.6 nm and this increased to only 8.4 nm for the 10 bilayer film; i.e., the roughness value is much less than the total thickness of the film.

The roughness increment per bilayer after the first bilayer was about 0.5 nm per bilayer, which is less than the roughness of the first bilayer and thus indicates highly smooth interfaces and the absence of aggregation within the multilayers. The surface roughness of the 10 bilayer film after heat treatment was 8.1 nm, which means that the heat treatment has only a minor effect on the film roughness. The PMMA/ZnO thin films are nonporous, as shown by the AFM image and the section analysis, figure 3. The final roughness value of 8.1 nm for the 10 bilayer film and a roughness increment of about 0.5 nm per bilayer indicate that these films are internally smooth and stratified and that there is no aggregation of either PMMA chains or ZnO QDs within the layers or at the interfaces between layers. This indicates the advantage and ease of incorporating nanoparticles inside a polymer matrix using spin-coating.

Thin PMMA/ZnO films absorb UV radiation at a wavelength of 351 nm, as indicated by the UV absorption spectra shown in figure 4. The absorption increases linearly with increasing number of bilayers, which supports the hypothesis that there is a constant loading of ZnO QDs in the film. UV absorption by the films takes place at the same wavelength as that of the dispersion of quantum dots, indicating that the quantum dots preserve their molecular state after incorporation in the polymer matrix. Moreover, the close packing of quantum dots as a result of the spin coating does not influence their absorption of radiation and hence the chemical state of the quantum dots. The absorption coefficient (α) can be calculated as $\alpha = A/t$, where A is the absorbance and t is the film thickness. The absorption coefficient (α) is related to the energy band gap (E_g) by: $\alpha = (h\nu - E_g)^{1/2}/h\nu$, where h is Planck's constant and ν is the frequency of the absorbed radiation.[32] if $(\alpha h\nu)^2$ is plotted versus $h\nu$ over the absorption wavelength range, the energy band gap (E_g) can be calculated by extrapolating the linear region of the curve to $\alpha = 0$. Applying this method, the band gap of the ZnO QDs is given at a value of 3.34 eV (see Figure S1 in the Supporting Information), very close to the value usually reported for ZnO crystals.[5] As previously reported,[24] ZnO nanoparticles in

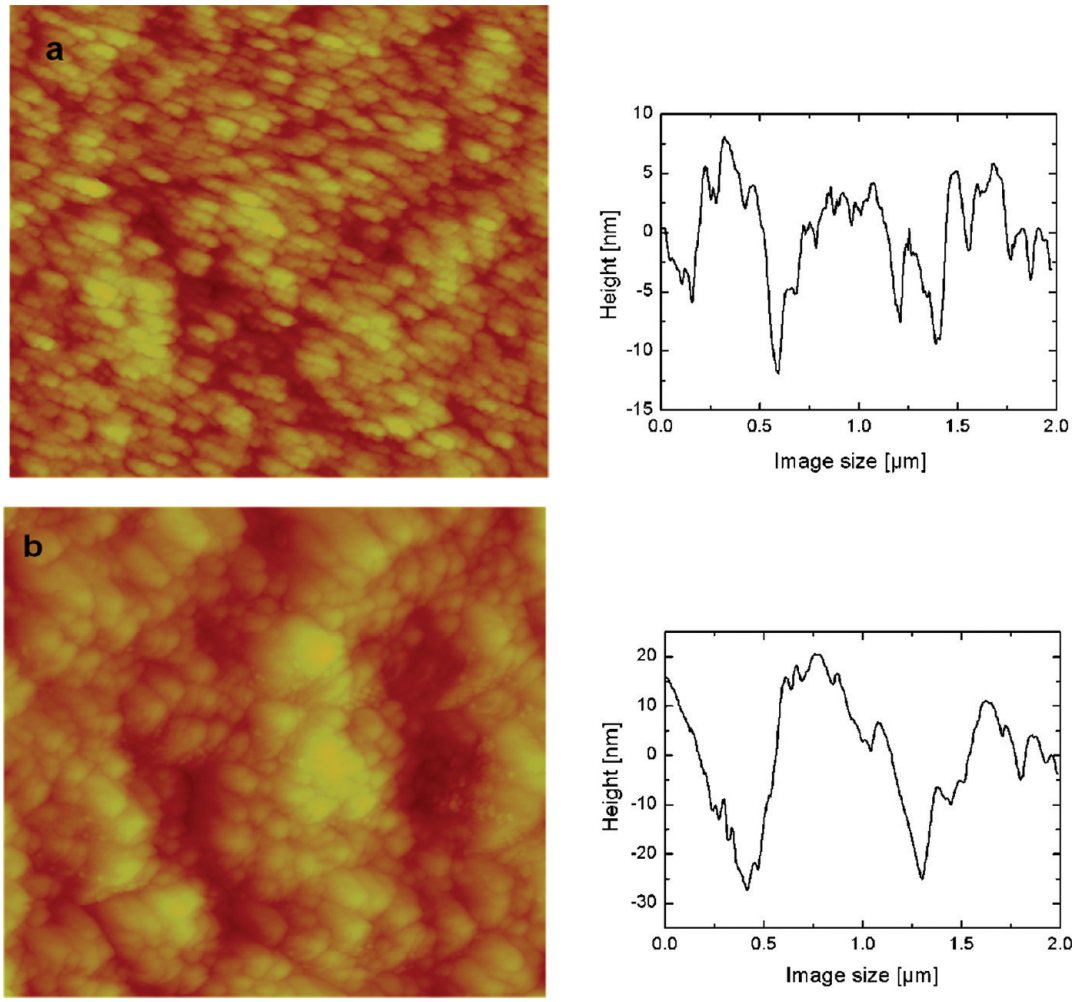

Figure 3. AFM height image and the corresponding section analysis of (a) 1 bilayer and (b) 10 bilayer films of PMMA/ZnO QDs. The rms surface roughness is 3.6 and 8.4 nm for the one and ten bilayer films, respectively.

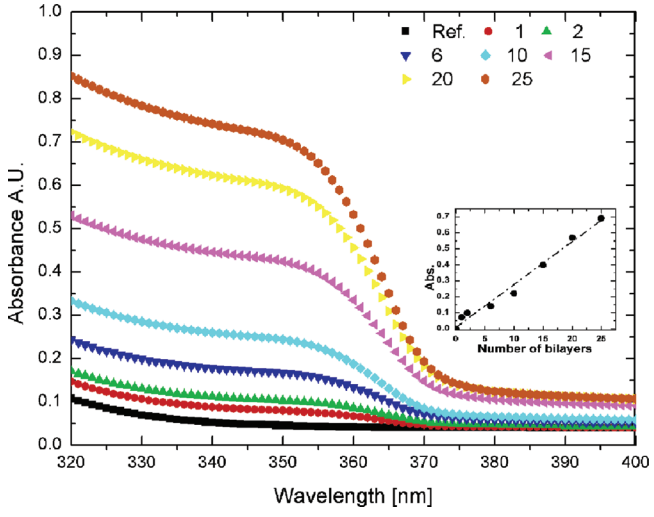

Figure 4. UV absorption spectra of PMMA/ZnO QDs thin films having 1−25 bilayers. The reference is a clean glass substrate. The inset show the absorbance of thin films at 351 nm plotted versus the number of bilayers after normalization with respect to the absorbance of the glass substrate.

multilayered polymer films exhibit the same value of the band gap as when they are dispersed in the liquid state.

The transmission in the UV region shows the same trend as that of the absorption. The transmission is damped starting at a wavelength of 371, figure 5, which is the absorption edge of the ZnO QDs, with a maximum damping at 351 nm, which is the maximum of the absorption shoulder of the ZnO QDs. Transmission at wavelengths lower than 280 nm is blocked by glass as well as PMMA, which also absorbs radiation in this range. Thus transmission is blocked over a broad range of wavelengths starting close to 400 nm at the edge of the visible region and extending throughout the UV regions. Apparently, thin films of PMMA and ZnO QDs could be applied efficiently as UV-blocking materials. Moreover, the incorporation of the QDs in the polymer matrix using the rather facile method of spin-coating has proved efficient in delivering stable thin films with a high degree of transparency and UV-blocking properties.

Transparency in the visible region is a valuable feature of this system compared to other UV-blocking materials which exhibit limited transparency in the visible region.[10,19] Here, transmission in the visible region is slightly reduced with increasing number of bilayers but is constant over the whole visible range extending even into the near IR region. Thus, a combination of ZnO QDS and PMMA in such thin films built up by spin-coating provides a broad-band UV-blocking in addition to a broad-band transparency in the visible regime and extending to

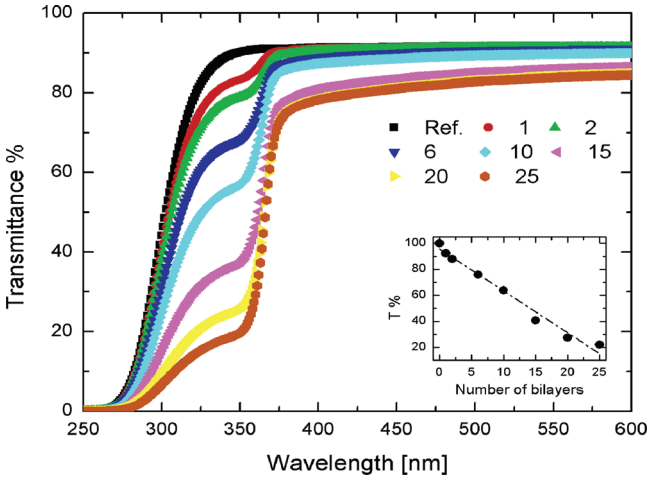

Figure 5. UV−vis transmission spectra of PMMA/ZnO QDs thin films on glass substrate. The inset plot shows the normalized transmission versus the number of bilayers at 351 nm. Transmission is blocked over the entire UV region, whereas it was only slightly reduced in the visible region.

the near IR region and the optical performance of these thin films can easily be tuned by choosing the number of bilayers.

Both the absorption and transmission properties of the thin films were investigated after heat treatment at 100 °C for 1 h. UV−vis spectra show that the heat treatment had no observable effect on either absorption or transmission. This indicates that the role of the heat treatment was limited to the removal of solvent and the introduction of homogeneity into the film, as indicated by the slight decrease in surface roughness of the 10 bilayer films with no effect on the chemical or molecular states of the QDs in the film. The absorption and transmission of UV radiation by the thin film can be tuned by controlling the number of bilayers, as shown in figures 4 and 5. To confirm this, figure 6 shows that the absorption of UV radiation can be tuned by controlling the ratio of ZnO QDs in a single layer of a mixture of ZnO QDs and PMMA. It is also shown that PMMA and glass have the same absorption spectra in the selected area of radiation. At wavelengths ≤290 nm both show the same absorption spectra, so that UV radiation at these wavelengths is blocked by both materials. In addition, there is a slight increase

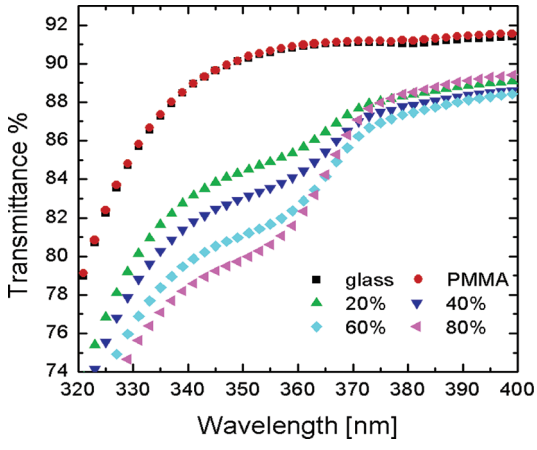

Figure 6. Transmittance of UV radiation through a single layer of a mixture of PMMA and ZnO QDs with different proportions of ZnO QDs.

in transmission, about 1%, in the visible region in the case of the 80% ZnO QDs content. Actually, this slight increase in transmission may be due to the higher porosity of this single layer when the content of ZnO QDs was increased. This porosity is due to the increased concentration of vicinities between QDs that are not coated with PMMA as its concentration has decreased.

The transmission of UV radiation can be reduced by increasing the proportion of ZnO QDs in the single layer of PMMA/ZnO QDs. With 80% of ZnO QDS, the transmission has decreased to a value of 80% whereas the transmission of glass or PMMA is 91%, at a wavelength of 351 nm.

The results obtained by ellipsometry, AFM and UV absorption spectra revealed that the ZnO QDs exist as a monolayer inside the multilayer and that they keep their molecular and chemical properties. Figure S2 in the Supporting Information shows that the ZnO QDs keep their quantum state as they still exhibit photoluminescence at the same wavelength as the dispersion, indicated by a green fluorescence when imaged by a confocal microscope at the excitation wavelength of 350 nm. The confocal image shows a projection of 36 confocal planes. The density of dots per confocal plane is limited but the image shows that it is possible to image the fluorescence emitted by QDs inside a polymer matrix of this small size. Figure S2 shows a 20% PMMA/ZnO QDs single layer indicating the high probability of fluorescence detection by this system. This is shown for the first time to the best knowledge of the authors.

As shown in Figure 5, the PMMA/ZnO QDs thin films are characterized by a high transparency that does not drop below 80% anywhere in the visible region. This high transparency is indicated in Figure 7, which shows a photograph of an image

Figure 7. Transparency of the PMMA/ZnO QDs thin films indicated by a photograph showing from left to right: a bare image, an image covered with a glass slide with 10 PMMA/ZnO QDs bilayers, and an image covered with a glass slide of 20 PMMA/ZnO QDs bilayers.

beside the same image covered with glass slides coated with 10 and 20 bilayers from left to right, respectively. The visual transparency is slightly dependent on the number of bilayers.

Contact angle measurements, Figure 8, gave values of 12°, 70° and 67° for a bare glass substrate, a PMMA layer and 10 bilayers of PMMA/ZnO QDs, respectively. The PMMA/ZnO

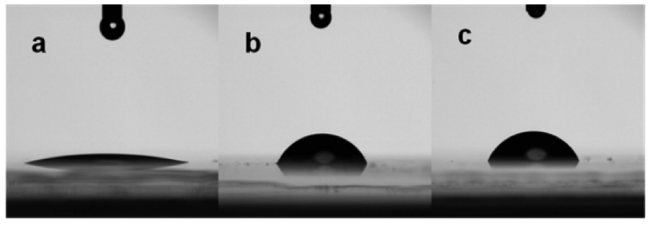

Figure 8. Contact angles of a water droplet on the surface of (a) bare glass, (b) a single PMMA layer, (c) 10 bilayers of PMMA/ZnO QDs.

dx.doi.org/10.1021/am300243u | ACS Appl. Mater. Interfaces 2012, 4, 2920−2925

QDs films are hydrophobic and this hydrophobicity is attributed mainly to the presence of PMMA. Nevertheless, the ZnO QDs also contribute to the hydrophobicity, since they are coated with oleic acid. Heat treatment had a minor effect on the contact angle as indicated by a decrease in the contact angle of water on a PMMA monolayer from 70 to 65° and on the 10 bilayer PMMA/ZnO QDs from 67 to 65° after heating for 1 h at 100 °C.

CONCLUSIONS

UV-blocking highly transparent thin films have been prepared as multilayers of ZnO QDs and PMMA using the spin-coating technique. It has been shown that the spin-coating technique is highly effective in building up smooth, stratified and homogeneous thin films. The thickness and morphology of the films indicate the build-up of consecutive PMMA and ZnO QDs layers of defined thickness and close-packing on the surface. The ZnO QDs retain their chemical and quantum properties through the build-up process, as shown by their UV absorption and photoluminescence emission. The UV-blocking films prepared in this work exhibit a high degree of transparency over the entire visible range, which is an advantage over the previously prepared nanocomposites that showed some degree of opacity. The method is facile, applicable to a wide range of surfaces and would require only a low energy input if applied on an industrial scale.

ASSOCIATED CONTENT

Supporting Information

Figures S1 and S2, this material is available free of charge via the Internet at http://pubs.acs.org.

AUTHOR INFORMATION

Corresponding Author

*E-mail: eita@kth.se. Tel.:+ (46) 8 7908148. Fax: + (46) 8 7909072.

Notes

The authors declare no competing financial interest.

REFERENCES

(1) *Encyclopedia of Applied Spectroscopy*; Andrews, D. L., Ed.; , Wiley-VCH Verlag: Weinheim, Germany, 2009; pp1−26,.
(2) Ries, G.; Heller, W.; Puchta, H.; Sandermann, H.; Seidlitz, H. K.; Hohn, B. *Nature* **2000**, *406*, 98.
(3) Li, S.; Lin, M. M.; Toprak, M. S.; Kim, D. K.; Muhammed, M. *Nano Reviews* **2010**, *1*, 1.
(4) Balazs, A. C.; Emrick, T.; Russell, T. P. *Science* **2006**, *314*, 1107.
(5) Srikant, V.; Clarke, D. R. *J. Appl. Phys.* **1998**, *83*, 5447.
(6) Thomas, D. G. *J. Phys. Chem. Solids* **1960**, *15*, 86.
(7) Hengehold, R. L.; Almassy, R. J.; Pedrotti, F. L. *Phys. Rev. B* **1970**, *1*, 4784.
(8) Pankove, J. I.; *Optical Processes in Semiconductors*; Dover:New York, 1971.
(9) Sun, D.; Miyatake, N.; Sue, H.-J. *Nanotechnology* **2007**, *18*, 215606.
(10) Paramo, J. A.; Strzhemechny, Y. M.; Anžlovar, A.; Žigon, M.; Orel, Z. C. *J. Appl. Phys.* **2010**, *108*, 023517.
(11) Lee, D. C.; Jang, L. W. *J. Appl. Polym. Sci.* **1996**, *61*, 1117.
(12) Kim, T. H.; Jang, L. W.; Lee, D. C.; Choi, H. J.; John, M. S. *Macromol. Rapid Commun.* **2002**, *23*, 191.
(13) Dirix, Y.; Bastiaansen, C.; Caseri, W.; Smith, P. *J. Mater. Sci.* **1999**, *34*, 3859.
(14) Dirix, Y.; Darribère, C.; Heffels, W.; Bastiaansen, C.; Caseri, W.; Smith, P. *Appl. Opt.* **1999**, *38*, 6581.
(15) Veinot, J. G. C.; Galloro, J.; Pugliese, L.; Pestrin, R.; Pietro, W. *J. Chem. Mater.* **1999**, *11*, 642.
(16) Park, J.; An, K.; Hwang, Y.; Park, J.-G.; Noh, H.-J.; Kim, J.-Y.; Park, J.-H.; Hwang, N.-M.; Hyeon, T. *Nat. Mater.* **2004**, *3*, 891.
(17) Sooklal, K.; Hanus, L. H.; Ploehn, H. J.; Murphy, C. J. *Adv. Mater.* **1998**, *10*, 1083.
(18) Chen, Q.; Schadler, L. S.; Siegel, R. W.; Irven, G. C. *Proc. SPIE* **2003**, *5222*, 158.
(19) Li, S.; Toprak, M. S.; Jo, Y. S.; Dobson, J.; Kim, D. K.; Muhammed, M. *Adv. Mater.* **2007**, *19*, 4347.
(20) Znaidi, L.; Soler Illia, G. J. A. A.; Benyahia, S.; Sanchez, C.; Kanaev, A. V. *Thin Solid Films* **2003**, *428*, 257.
(21) Kulyk, B.; Kapustianyk, V.; Tsybulskyy, V.; Krupka, O.; Sahraoui, B. *J. Alloys Compd.* **2010**, *502*, 24.
(22) Tu, Y.; Zhou, L.; Jin, Y. Z.; Gao, C.; Ye, Z. Z.; Yang, Y. F.; Wang, Q. L. *J. Mater. Chem.* **2010**, *20*, 1594.
(23) Chen, Q.-H.; Shi, S.-y.; Zhang, W.-g. *Colloid Polym. Sci.* **2009**, *287*, 533.
(24) Eita, M.; Wågberg, L.; Muhammed, M. *J. Phys. Chem. C* **2012**, *116*, 4621−4627.
(25) Murray, C. B.; Kagan, C. R.; Bawendi, M. G. *Annu. Rev. Mater. Sci.* **2000**, *30*, 545.
(26) Bruchez, M., Jr; Moronne, M.; Gin, P.; Weiss, S.; Alivisatos, A. P. *Science* **1998**, *281*, 2013.
(27) Kiel, M.; Mitzscherling, S.; Leitenberger, W.; Santer, S.; Tiersch, B.; Sievers, T. K.; Möhwald, H.; Bargheer, M. *Langmuir* **2010**, *26*, 18499.
(28) Moussodia, R.-O.; Balan, L.; Merlin, C.; Mustin, C.; Schneider, R. *J. Mater. Chem.* **2010**, *20*, 1147.
(29) Jin, B. J.; Im, S.; Lee, S. Y. *Thin Solid Films* **2000**, *366*, 107−110.
(30) Egelhaaf, H. −J.; Oelkrug, D. *J. Cryst. Growth* **1996**, *161*, 190−194.
(31) Van Heusden, K.; Seager, C. H.; Warren, W. L.; Tallant, D. R.; Voigt, J. A. *Appl. Phys. Lett.* **1996**, *68*, 403−405.
(32) Tauc, J. *Amorphus and Liquid Semiconductors*; Plenum: London, 1974.